ARCHIVES OF ELECTRICAL ENGINEERING VOL. 60(2), pp. 187-195 (2011)

DOI 10.2478/v10171-011-0018-3

Numerical analysis of hysteresis loss in pulse transformer

WIESŁAW ŁYSKAWIŃSKI, PIOTR SUJKA, WOJCIECH SZELĄG, MARIUSZ BARAŃSKI

Institute of Electrical Engineering and Electronics
Poznan University of Technology
Piotrowo 3a, 60-965 Poznań, Poland

e-mail: {Wieslaw.Lyskawinski /Piotr.Sujka /Wojciech.Szelag /Mariusz.Baranski}@put.poznan.pl

(Received: 02.07.2010, revised: 10.12.2010)

Abstract: In the paper, the mathematical model of coupled electromagnetic and thermal phenomena in the pulse transformer taking into account the magnetic hysteresis is presented. For the mapping of magnetic hysteresis, Jiles-Atherton model is applied. In order to solve field equations, the finite element method (FEM), "step-by-step" procedure and Newton-Raphson algorithm are used. Software elaborated on this basis is used for analysis of hysteresis loss in the core. Selected results of investigations are shown.

Key words: hysteresis loss, pulse transformer, coupled electromagnetic-thermal phenomena, Jiles-Atherton model

1. Introduction

To analyze the operating conditions of a pulse transformer thoroughly, a mathematical model taking into account all phenomena which are essential to describe its behavior is needed. Among other things, an accurate representation of the phenomenon of magnetic hysteresis as well as the calculation of power losses in the core connected therewith present many problems. Usually the phenomenon of magnetic hysteresis is omitted during the field analysis of electromagnetic converters, and the magnetic properties of a ferromagnetic material are described by means of a unique magnetization curve. Such a simplification can not be applied when the hysteresis loss in the core is determined. The influence of the temperature of sub-assemblies of the converter on the course of transient phenomena is rarely taken into consideration [1].

In the paper, a field model taking into account the influence of magnetic hysteresis and temperature on the course of transient electromagnetic phenomena has been proposed to analyze a pulse transformer operating at high frequency. The Jiles-Atherton model has been applied to represent the hysteresis. The equations describing the electromagnetic and thermal

fields were solved together using FEM. The elaborated algorithm and software for the analysis of the coupled phenomena in a pulse transformer was used to determine hysteresis loss.

2. Jiles-Atherton hysteresis model

In the Jiles-Atherton model [2, 10], it is assumed that the magnetization M of a material is caused by the factors representing reversible processes M_{rev} and irreversible processes M_{irr} occurring during the magnetization of the core

$$M = M_{rev} + M_{irr} \tag{1}$$

in the above equation, the irreversible processes occurring in the course of magnetization are described by a differential equation

$$\frac{\mathrm{d}M_{irr}}{\mathrm{d}H} = \frac{M_{an} - M_{irr}}{k\delta - \alpha(M_{an} - M_{irr})}, \tag{2}$$

where $\delta = \mathrm{sgn}\,\mathrm{d}H/\mathrm{d}t$, M_{an} is a non-hysteresis magnetization curve

$$M_{an} = M_{sat}\left(\coth\frac{H + \alpha M}{a} - \frac{a}{H + \alpha M}\right). \tag{3}$$

In the above relations, k and α are the factors depending on material parameters, a is the shape factor, and the saturation magnetization is denoted by M_{sat}.

In the model, it is assumed that the reversible processes inside a material are described by the equation

$$M_{rev} = c\,(M_{an} - M_{irr}), \tag{4}$$

where c is the factor depending on the type of material.

By substituting (4) into (1) and then differentiating the achieved expression it is obtained as follows

$$\frac{\mathrm{d}M}{\mathrm{d}H} = \frac{(1-c)\,(M_{an} - M_{irr})}{k\delta - \alpha(M_{an} - M_{irr})} + c\frac{\mathrm{d}M_{an}}{\mathrm{d}H}. \tag{5}$$

When modeling the voltage-excited magnetic field, it is necessary to calculate the magnetic field strength intensity on the basis of magnetic flux density. In FEM algorithm magnetic flux density is determined using vector magnetic potential. Then, instead of the derivative of M with respect to the field intensity (5), its derivative with respect to the magnetic induction is determined by the following expression:

$$\frac{\mathrm{d}M}{\mathrm{d}B} = \frac{(1-c)\frac{\mathrm{d}M_{an}}{\mathrm{d}B_e} + \frac{c}{\mu_0}\frac{\mathrm{d}M_{an}}{\mathrm{d}H_e}}{1 + (1-\alpha)\left(\mu_0(1-c)\frac{\mathrm{d}M_{irr}}{\mathrm{d}B_e} + c\frac{\mathrm{d}M_{an}}{\mathrm{d}H_e}\right)}, \tag{6}$$

where μ_0 is air permeability, effective induction $B_e = \mu_0 H_e$ and induction $B = B_e - \mu_0 \alpha M + \mu M$.

In order to solve equations (5) and (6), i.e., to determine the magnetization M, numerical methods of solving differential equations, for example the difference methods or the Runge-Kutta method can be used.

3. Hysteresis loss determination algorithm

On account of the coupling of electromagnetic and heat effects in a pulse transformer it is to analyze these effects jointly [6]. In the paper, an axial symmetry transformer was analyzed. The cylindrical coordinate system r, z, β (Fig. 1) was used to describe the coupled. The equation of electromagnetic field written in this system has the form [5]

$$\frac{\partial}{\partial r}\left(\frac{1}{\mu l}\frac{\partial \varphi}{\partial r}\right) + \frac{\partial}{\partial z}\left(\frac{1}{\mu l}\frac{\partial \varphi}{\partial z}\right) = -\left(J + J_M - \frac{\gamma}{l}\frac{d\varphi}{dt}\right), \tag{7}$$

here $l = 2\pi r$, $\varphi = 2\pi r A_\beta$, where A_β is the auxiliary magnetic potential, $J = J(r, z)$ is the current density in the β – direction and $J_M = J_M(r, z)$ is the current density of the magnetization M, γ is the conductivity.

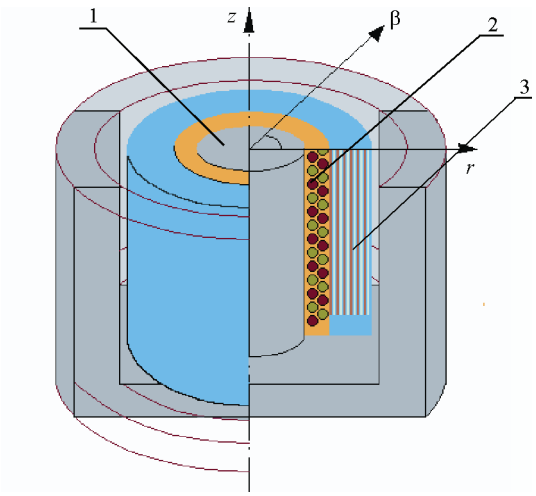

Fig. 1. Pulse transformer 1 – ferrite core, 2 – primary winding, 3 – secondary winding

The equation (7) should be solved simultaneously with the equations of electric circuits

$$\mathbf{u} = \mathbf{R}\mathbf{i} + \frac{d}{dt}\mathbf{\Psi} + \mathbf{L}_z \frac{d}{dt}\mathbf{i} + \mathbf{E}_z \int_0^t \mathbf{i}\, dt, \tag{8}$$

where $\mathbf{u}$ is the vector of supply voltages, $\mathbf{i}$ is the vector of loop currents, $\mathbf{R}$ is the matrix of loop resistances, $\mathbf{L}$ is the matrix of inductances, $\mathbf{\Psi}$ is the flux linkage vector calculated on the

basis of field distribution, $\mathbf{L}_z$, $\mathbf{E}_z$ are the inductance and elastance matrixes of the supply system, respectively.

The heat effects are described by means of the equation [1, 11]

$$\frac{1}{r}\frac{\partial}{\partial r}\left(k_r r \frac{\partial \vartheta}{\partial r}\right) + \frac{\partial}{\partial z}\left(k_z \frac{\partial \vartheta}{\partial z}\right) = c_W g \frac{\partial \vartheta}{\partial t} - p, \tag{9}$$

where p is density of power losses, ϑ is the temperature, k_r, k_z are heat conductivities, g is the material density, c_W is the specific heat.

The solution of the equation (9) is uniquely determined by the boundary conditions of second and third kind on the external surfaces of windings and core [8]. It was assumed that the heat flux q penetrating through the external surface is proportional to the temperature difference between this surface and the environment, i.e., $q = k(\partial \vartheta / \partial n) = c_p(\vartheta_{ot} - \vartheta)$, where c_p is the equivalent coefficient of giving up the heat.

The density of power losses p in the equation (9) is determined on the basis of the time and spatial distribution of the current density j from the relation

$$p = \frac{J^2}{\gamma}. \tag{10}$$

The equations (7), (8), (9) are coupled by the conductivity $\gamma(\vartheta)$ and permeability $\mu(B, \vartheta)$ of materials as well as the density of power losses p. For this reason they should be solved simultaneously. To solve these equations, the method of finite elements and the method „step-by-step" were used [7, 3]. As a result of the discretization of space and time a system of nonlinear algebraic equations is obtained from the field equation

$$\begin{bmatrix} \mathbf{M}_n & -\mathbf{N} \\ -\mathbf{N}^{\mathrm{T}} & -\Delta t \mathbf{Z} \end{bmatrix} \begin{bmatrix} \boldsymbol{\varphi}_n \\ \mathbf{i}_n \end{bmatrix} = \begin{bmatrix} (\Delta t)^{-1} \mathbf{G}(1-\mathbf{K})\boldsymbol{\varphi}_{n-1} + \boldsymbol{\theta}_n \\ -\Delta t \mathbf{u}_n + \tilde{\boldsymbol{\psi}}_{n-1} \end{bmatrix}, \tag{11}$$

$$\mathbf{G}_{\vartheta n}\, \vartheta_n + (\Delta t)^{-1} \mathbf{A}_w\, \vartheta_n = \mathbf{Y} + (\Delta t)^{-1} \mathbf{A}_w\, \vartheta_{n-1}, \tag{12}$$

where:

$$\mathbf{M}_n = \mathbf{S}_n + (\Delta t)^{-1} \mathbf{G}(1-\mathbf{K}), \qquad \mathbf{Z} = \mathbf{R} + \Delta t\, \mathbf{E}_z + (\Delta t)^{-1} \mathbf{L}_z,$$

$$\tilde{\boldsymbol{\psi}}_{n-1} = -\mathbf{N}^{\mathrm{T}} \varphi_{n-1} - (\Delta t)^{-1} \mathbf{L}_z \mathbf{i}_{n-1} + \Delta t\, \mathbf{u}_{cn-1},$$

n denotes the number of time-step, Δt is the time-step length, φ is the vector of nodal potentials, $\mathbf{N}^{\mathrm{T}}$ is the matrix that transforms the potentials φ into the flux linkages with the windings, $\mathbf{G}$ is the matrix of conductances of elementary rings formed by mesh, $\mathbf{S}$ is the stiffness matrix, $\mathbf{K}$ is the matrix consisting of diagonally placed sub-matrixes whose elements equal the ratio of the cross-section area of the fibre assigned to a given node to the cross-section area of the wire in this node, $\mathbf{u}_{cn-1}$ is the vector of the voltage on the capacitances at the $n-1$ time step $\mathbf{G}_{\vartheta n}$ is the matrix of heat conductivity, $\mathbf{A}_W$ is the matrix of heat capacities, $\mathbf{Y}$ is the vector of the nodal heat, θ_n is the vector with elements dependent on the magnetization M.

In order to formulate equation (6) of the discrete model of electromagnetic phenomena it has been assumed that the magnetic properties of a ferromagnetic material are described by the equation $H = B/\mu_0 - M$, whereas the magnetization M is determined on the basis of magnetic induction from the inverse Jiles-Atherton model [4, 9]. In order to solve the system of non-linear coupled equations (11) and (12), the block relaxation method and the Newton-Raphson algorithm were used.

The hysteresis power loss in the core is determined by the following expression

$$\Delta P_h = f \sum_{i=1}^{lr} w_{hi} V_i, \tag{13}$$

where lr is the number of the finite elements digitizing the core, f is the frequency, V_i is the volume of the i-th element in which the density of energy being lost during one magnetization cycle

$$w_{hi} = \sum_{n=1}^{tn} \frac{H^n + H^{n-1}}{2}\left(B^n - B^{n-1}\right), \tag{14}$$

where B^n, B^{n-1}, H^n, H^{n-1} are the magnetic flux density and intensity, respectively, in the i-th element obtained for the n-th and $(n-1)$-th time step, and tn is the number of time steps within one magnetization period of the core.

4. Calculation results

On the basis of the presented algorithm of solving the equations of the discrete model, the software to simulate and visualize transient electromagnetic and heat phenomena in a pulse transformer, taking into account magnetic hysteresis, has been elaborated. This software was used to analyze hysteresis loss. A considered pulse transformer ETD 44 type is shown in Fig. 2.

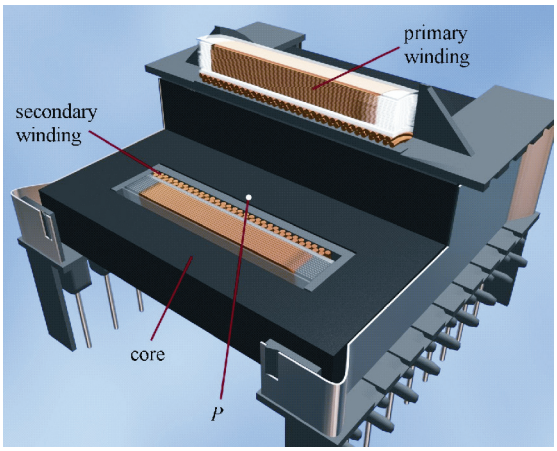

Fig. 2. Pulse transformer

The core was made from ferrite F867. In order to take into account the influence of the temperature on magnetic properties of ferrite F867, the hysteresis loops family was determined. The selected results of measurements are shown in Fig. 3. The parameters required in the Jiles-Atherton model for a few temperatures were determined on the basis of the measured hysteresis loops. The parameters of the Jiles-Atherton model for these temperatures were estimated by minimizing the error described by equation

$$\varepsilon = \frac{1}{N}\sum_{j=1}^{N}\left(B_{j\,\mathrm{sim}} - B_{j\,\mathrm{meas}}\right)^2, \tag{15}$$

where N is the number of measuring points, $B_{j\,\mathrm{meas}}$ and $B_{j\,\mathrm{sim}}$ are respectively measured and calculated magnetic flux densities.

In Figure 3, the loops of the hysteresis obtained from the Jiles-Atherton model are also shown. A considerable agreement between results of measurements and calculations was obtained. For the purpose of determining magnetic properties of the core for any temperature, a linear approximation was used.

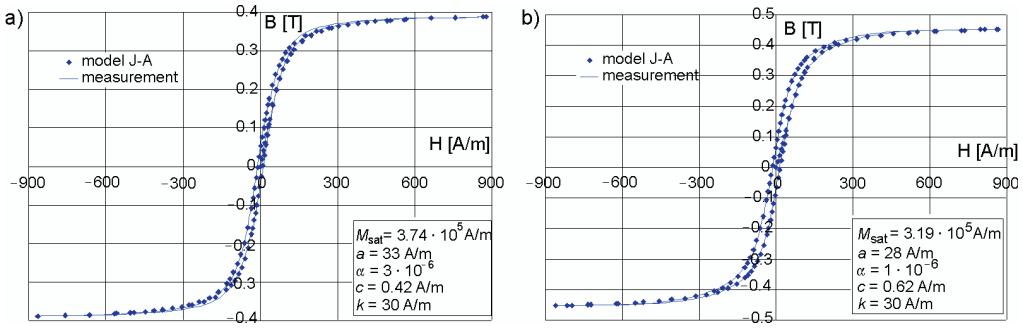

Fig. 3. Measured and modelled hysteresis loops for (a) 30°C and (b) 90°C

A work of the transformer has been analyzed at different shapes of the course and the frequency of supply voltage. During the simulations, the ratio of voltage amplitude to frequency was constant. The initial instant of connecting supply voltage was selected so that the steady state could be obtained as soon as possible. Therefore the duration of calculations has been shortened considerably. Exemplary hysteresis loops obtained as a result of the calculations are shown in Fig. 4. They present the relationships $B(H)$ determined at the point P of the middle column of the core (Fig. 2) at the nominal load of the transformer supplied with pulse and sinusoidal voltage with a frequency of 100 kHz as well as pulse voltage with a frequency of 200 kHz.

It was assumed that the transformer was supplied with rectangular voltage pulses of negative and positive polarization. In order to obtain the constant value of rectified voltage at the system output was achieved by modulating the pulse width in the range of 5 to 45%.

The influence of frequency on hysteresis losses at pulse and sinusoidal supply was examined. The selected results are shown in Fig. 5.

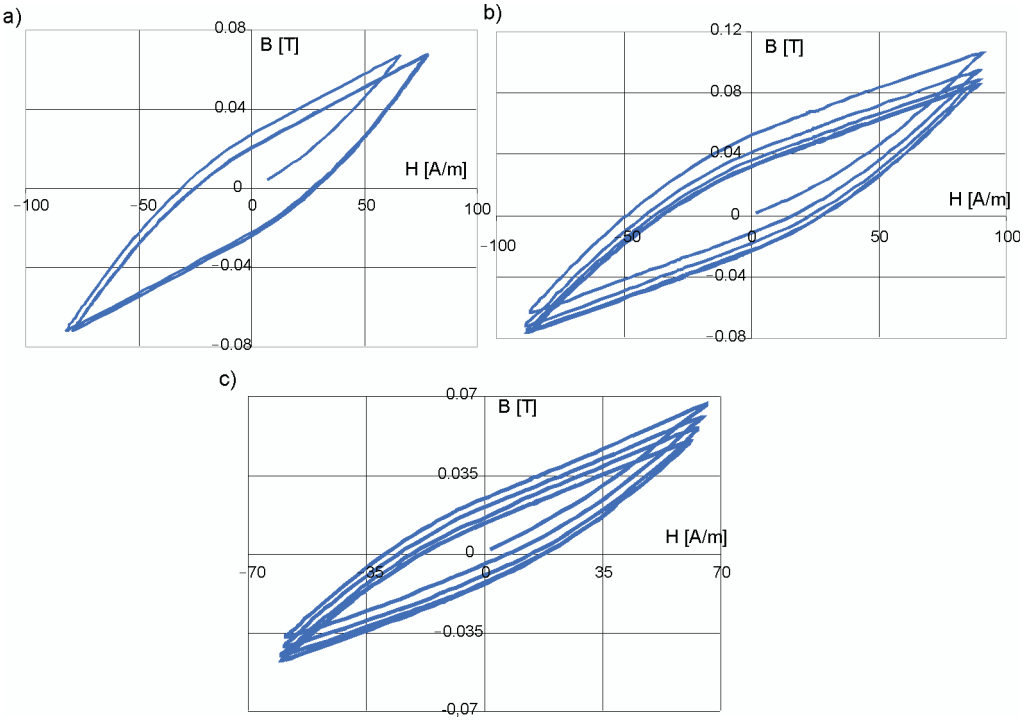

Fig. 4. Hysteresis loops determined for: a) sinusoidal supply voltage ($f = 100$ kHz, $\vartheta = 56.8^{\circ}$C), b) impulse supply voltage ($f = 100$ kHz, $\vartheta = 60.5^{\circ}$C), c) impulse supply voltage ($f = 200$ kHz, $\vartheta = 53.1^{\circ}$C.)

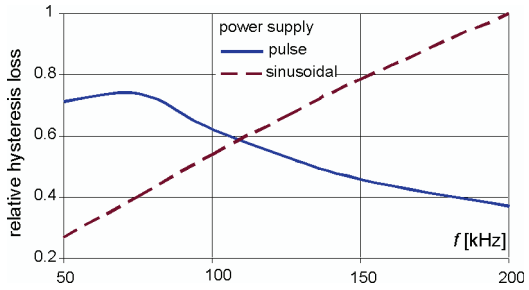

Fig. 5. Relative hysteresis loss in the core with respect to frequency

It follows from them that in the examined range of pulse supply, the losses increase slightly with an increase in frequency at the beginning, and then they decrease quickly. The hysteresis losses have a maximal value when the pulse-duty factor is equal to 45%. From the performed analysis, it results that the pulse-duty factor k_i needed to obtain the set voltage value at the transformer output decreases with an increase in frequency (Fig. 6). For this reason, the current in the windings, and so also the magnetic field intensity in the core, increases to a more and more little value with an increase in frequency. The effect was that the hysteresis loop and also hysteresis losses decrease with an increase in frequency and the

decreasing pulse-duty factor. But for a frequency less than 65 kHz, after the pulse-duty factor has achieved the boundary value of 45% (Fig. 6), the losses in the core decrease because of the frequency decreases with a slight increase of the surface area of hysteresis loop.

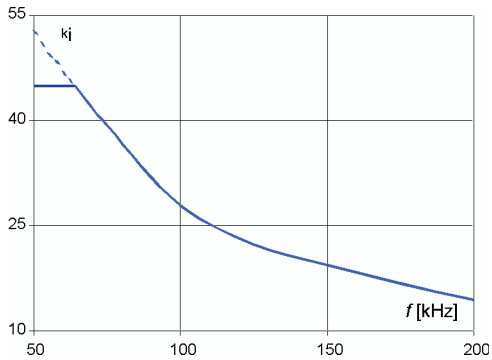

Fig. 6. PWM factor frequency characteristics

5. Conclusions

In the paper, the field model of a pulse transformer taking into account the influence of magnetic hysteresis on the course of coupled electromagnetic and heat phenomena have been presented. The Jiles-Atherton model was used to represent hysteresis. The elaborated algorithm and software for the analysis of coupled electromagnetic and heat phenomena, taking into account magnetic hysteresis, were used among other things, to examine the influence of the course shape and frequency of supply voltage on the hysteresis losses of a transformer. In the authors' opinion, the elaborated software can be useful for designing pulse transformers and the analysis of hysteresis power losses.

References

[1] Driesen J., *Coupled electromagnetic-thermal problems in electrical energy transducers.* Katholieke Universiteit Leuven, Leuven (2000).
[2] Ivanyi A., *Hysteresis models in electromagnetic computation.* Akademiai Kiadó, Budapest 1997.
[3] Jedryczka C., Sujka P., Szelag W., *The influence of magnetic hysteresis on magnetorheological fluid clutch operation.* COMPEL – The International Journal for Computation and Mathematics in Electrical and Electronic Engineering 28(3): 711-721 (2009).
[4] Nowak L., *Simulation of the dynamics of electromagnetic driving device for comet ground penetrator*. IEEE Transactions on Magnetics 34(5): 3146-3149 (1998).
[5] Leite J.V., Sadowski N., Kuo-Peng P. et al., *The inverse Jiles-Atherton model parameter identification.* IEEE Transactions on Magnetics 39(3): 1397-1400 (2003).
[6] Łyskawinski W., *Field approach to power loss analysis of pulse transformer.* Archives of Electrical Engineering LVI(2): 103-114 (2007).
[7] Łyskawinski W., Szelag W., *Analysis of eddy current influence on transient thermal phenomena in pulse transformer.* Poznań University of Technology Academic Journals, Computer Applications in Electrical Engineering 60: 115-120 (2009).

[8] Rappaz M., Bellem M., Deville M., *Numerical modeling in materials science and engineering.* Springer, Berlin (2003).
[9] Sadowski N., Batistela N.J., Bastos J.P.A., Lajoie-Mazenc M., *An inverse Jiles-Atherton model to take into account hysteresis in time-stepping finite element calculations.* IEEE Transactions on Magnetics 38(2): 897-900 (2002).
[10] Szczygłowski J., *Influence of eddy currents on magnetic hysteresis loops in soft magnetic material.* Journal of Magnetism and Magnetic Materials 223(1): 97-102 (2001).
[11] Szelag W., *Finite element analysis of the magnetorheological fluid brake transients.* COMPEL – The International Journal for Computation and Mathematics in Electrical and Electronic Engineering 23(3): 758-766 (2004).